

## Radioiodination and Biological Evaluation of Tizanidine as a Potential Brain Imaging Agent

M.A. Mourad<sup>a</sup>, H. Abd El-Aziz<sup>b</sup>, A.M. Amin<sup>b</sup>, G.G. Mohamed<sup>c</sup> and S.A. Abo El-Enein<sup>d</sup>

<sup>(a)</sup>Centre of Radiation Oncology and Nuclear Medicine, Kasr Al-Ainy, Cairo, Egypt

<sup>(b)</sup>Labeled Compounds Department, Hot Labs Center, Atomic Energy Authority, Cairo, Egypt

<sup>(c)</sup>Chemistry Department, Faculty of Science, Cairo University, 12613, Giza, Egypt

<sup>(d)</sup>Chemistry Department, Faculty of Science, Ain Shams University, Cairo, Egypt

Received 1<sup>st</sup> May 2017  
Accepted 1<sup>st</sup> Jan. 2018

Labeling was carried out by direct iodination of tizanidine (100 µg) with radioiodine (<sup>125</sup>I) in a fast single step at room temperature, to produce <sup>125</sup>I-tizanidine (<sup>125</sup>I-TZN). 50 µg chloramine-T (CAT) was used as an oxidizing agent to oxidize the iodide ion to the iodonium ion, at neutral pH = 7 within 15 min. A high radiochemical yield of 92.8 % ± 0.1 was obtained. <sup>125</sup>I-TZN was stable for 2 h without detection of any by-products in the reaction mixture. The partition coefficient value of <sup>125</sup>I-TZN was 2.21 ± 0.02, showing that it is very lipophilic and can easily cross the blood brain barrier. Biodistribution studies and *in vivo* imaging showed that the initial brain uptake correlated fairly well with the brain-binding affinity of the compound. The brain uptake of <sup>125</sup>I-TZN was as high as 5.2 % and 8.0 % in biodistribution studies and *in vivo* imaging at 120 min post injection, respectively. Thus, <sup>125</sup>I-TZN is promising in radioreceptor assays for brain imaging.

**Keywords:** Radioiodination - Tizanidine - Biodistribution- Brain Imaging - SPECT

### Introduction

Nuclear medicine imaging involves the detection and spatial mapping of the radiation emitted by a radiopharmaceutical labeled with a specific radionuclide. The objectives of a nuclear medicine scan of the brain may include, for example, the detection of lesions, the evaluation of regional cerebral blood flow (rCBF), or the quantitative determination of a particular metabolic process such as the rate of regional glucose utilization [1]. The development of emission tomography is a good example of the fusion of a number of scientific and medical disciplines to produce an effective imaging technique. There are two different techniques of emission tomography:

positron emission tomography (PET), based on radionuclides which decay by positron emission, and single photon

emission computed tomography (SPECT) which is based on radionuclides which emit gamma rays or X-rays. While PET has some inherent technical advantages over SPECT, the economic reality dictates that SPECT is usually the only technique available in routine clinical practice. Recent innovations in the design of multi-head SPECT systems, which allow them to detect positron-emitting radionuclides, have diminished the sharp distinction between the two techniques [2].

Corresponding Author: [mai.adel89@gmail.com](mailto:mai.adel89@gmail.com)

DOI: [10.21608/ajnsa.2018.2178.1017](https://doi.org/10.21608/ajnsa.2018.2178.1017)

© Scientific Information, Documentation and Publishing Office (SIDPO)-EAEA

Isotopes of iodine have, for decades, played a fundamental role in biomedical research and in clinical practice. The diversity of decay schemes available for the various isotopes of iodine has allowed a wide range of medical applications. For example, iodine-125 is a convenient radionuclide for *in vitro* applications because it has a long half-life (about 59 days) and emits low-energy photons (35 keV), while  $^{131}\text{I}$  is more suitable for *in vivo* imaging because of its high-energy gamma radiation (364 keV) [3]. Moreover, iodine-123 has the decay properties required for diagnostic *in vivo* studies [4]. Synthetic approaches for the radioiodination of compounds generally follow established conventional chemical methods [5]. Direct methods involve the use of CAT [6], iodogen [7] and lactoperoxidase [8]. Indirect methods, which have been utilized, include conjugation of the radioiodinating reagent such as Bolton-Hunter reagent [9], N-succinimidyl para-iodobenzoate [10] and radioiodinated tyramine [11].

Tizanidine hydrochloride (5-chloro-4-(2-imidazolin-2-ylamino)-2,1,3-benzothiazol hydrochloride) belongs to the class of organic compounds known as benzothiadiazoles. These are heterocyclic aromatic compounds containing a benzene ring fused to a thiaziazole ring (Fig. (1)). TZN is a centrally acting  $\alpha_2$ -adrenergic agonist with an average blood-brain barrier penetration probability of 0.8592 [12], which is used as a systemic muscle relaxant. The present study deals with the iodine-125 labeling of TZN to obtain a novel agent for brain imaging. Factors affecting the labeling yield were studied in detail.

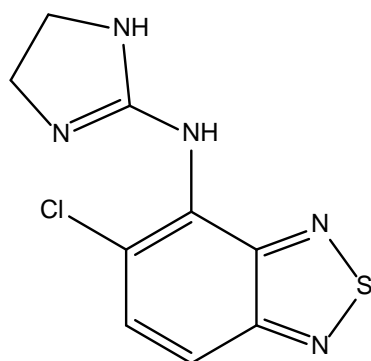


Fig. (1): Chemical structure of TZN

## Experimental

### Chemicals

*Arab J. Nucl. Sci. & Applic.* Vol. 51, No.2 (2018)

All chemicals and laboratory reagents used during this work were of the highest purity analytical grade. Double distilled water was used in all experiments. TZN was kindly supplied by the National Organization for Drug Control and Research (NODCAR), Giza, Egypt. CAT was purchased from Aldrich Chemical Company, China. Radioactive iodine-125 (NaI) with 370 MBq activity from Izotop Company, Budapest. Radioactive iodine-131 (NaI) with 1.85 GBq activity was supplied by the Radioisotope Production Facility, Egyptian Atomic Energy Authority, Egypt. Citric acid (pH 2 and 4), phosphate (pH 7) and bicarbonate (pH 9 and 11) buffers were prepared for pH adjustment. Silica gel thin-layer chromatography (SG-TLC) was purchased from Merck, Germany. Radioactivity was measured by means of a single detector  $\gamma$ -counter (Hidex model).

### Radiolabeling of TZN

Radiolabeling of TZN was carried out by adding a suitable concentration of TZN to an appropriate quantity of freshly prepared CAT and the pH of the reaction mixture was varied (pH 2-11) using different buffer systems. Carrier-free  $\text{Na}^{125}\text{I}$  was added to this mixture [13], followed by vortex and then the reaction mixture was kept in a water bath for different time intervals. The reaction was quenched by the addition of sodium thiosulfate solution [14].

### Determination of radiochemical yield

The radiochemical yield of the  $^{125}\text{I}$ -TZN was determined using aluminum-backed silica gel-60 sheet (20x20 cm). The SG-TLC strips (1.5 cm width, 14 cm length) were marked 2 cm from the base and lined into 1 cm fragments using a non-pointed pencil. A reaction product sample (5  $\mu\text{L}$ ) was spotted 5 times repeatedly with a micropipette, then the strip was developed in an ascending manner in a closed cylinder filled with chloroform-ethanol mixture (9:1 v/v). After complete development, the strips were dried, cut into 1 cm pieces and counted in a well-type  $\gamma$ -scintillation counter. The radiochemical yield was calculated as the mean value of three replicate measurements.

### Determination of radiochemical purity

The radiochemical purity of  $^{125}\text{I}$ -TZN was determined by direct injection of 5-10  $\mu\text{L}$ , of the reaction mixture at the optimum conditions for obtaining the highest radiochemical yield, into RP-

C18 column of a Shimadzu high performance liquid chromatography (HPLC) with methanol: acetonitrile: pH 6.6 phosphate buffer (15:40:45 v/v) as mobile phase using a UV detector operating at 307 nm. The mobile phase was fed at a rate of 1.0 mL/min. The fractions were collected and counted using NaI/Tl crystal connected to gamma counter [15].

#### *In vitro stability*

The reaction mixture was prepared in conditions which gave the highest radiochemical yield. The *in vitro* stability of  $^{125}\text{I}$ -TZN was studied at different time intervals (1, 2, 4, 8 and 24 h) and the radiochemical yield was calculated at each time.

#### *Lipophilicity*

The partition coefficient of  $^{125}\text{I}$ -TZN was determined in the system 1-octanol and phosphate buffer (0.025 mol/L at pH 7.4) at equal phase volumes. Experiments were performed in a centrifuge tube. The mixture was vortexed at room temperature for 1 min and then centrifuged at 5000 rpm for 5 min. After that, 100  $\mu\text{L}$  samples from each phase were pipetted into other test tubes and counted in a  $\gamma$ -counter. The measurement was repeated three times. The partition coefficient was expressed as log P according to the following equation [16]:

$$\text{Log } p_{\text{oct/buf}} = \text{Log} \left( \frac{[\text{solute}]_{\text{octanol}}}{[\text{solute}]_{\text{phosphate buffer}}} \right) \quad (1)$$

#### *In vivo biodistribution studies*

The study was approved by the Animal Ethics Committee, Labeled Compounds Department, and was in accordance with the guidelines set out by the Egyptian Atomic Energy Authority. The animals, normal Swiss Albino male mice (25-30 g), were intravenously injected with 200  $\mu\text{L}$   $^{125}\text{I}$ -TZN via the tail vein and kept alive in metabolic cage for different intervals of time under normal conditions. Three mice were used for each experiment. The mice were sacrificed at 10, 60, 120 and 240 min post injection. Samples of fresh blood, bones and muscles were collected in preweighed vials and counted. The weights of blood, bones and muscles were assumed to be 7, 10 and 40 % of the total body weight, respectively [17]. Radioactivity percentage in each tissue/organ was measured using  $\gamma$ -scintillation detector. The brain/blood ratio was calculated from the

corresponding percentage of the injected dose per gram (% ID/g) values.

#### *In vivo SPECT imaging*

Mice were anaesthetized by intravenous injection of diazepam (5  $\mu\text{L/g}$ ), then injected with the  $^{131}\text{I}$ -TZN compound (containing 37 MBq) via the caudal vein. Each mouse was positioned for imaging at the chosen time intervals (10, 60, 120 and 240 min). The mice were imaged in supine and feet first position with 180 head configuration for 10 min acquisition duration using high energy general all purpose-parallel (HEGAP-Par) collimator. The obtained images were planner with  $128 \times 128$  matrix.

## Results and Discussion

#### *Effect of substrate concentration*

The influence of TZN concentration on the percentage of radiochemical yield of  $^{125}\text{I}$ -TZN for 15 min at room temperature (about  $25 \pm 3$  °C) was investigated using 50  $\mu\text{g}$  CAT with 200  $\mu\text{L}$  phosphate buffer (pH 7) as shown in Fig. (2). The results indicate that the radiochemical yield increases with increasing the concentration of TZN till reaching  $92.8 \% \pm 0.1$  at 100  $\mu\text{g}$  TZN. Further increase in concentration, show a slight decrease in the percent of the radiochemical yield. This may be attributed to the fact that 100  $\mu\text{g}$  of TZN is enough to capture the entire generated iodonium ions as a result of the oxidation of the radioactive iodide ( $^{125}\text{I}$ ) at 50  $\mu\text{g}$  CAT [18].

#### *Effect of CAT concentration*

Radioiodination of organic molecules has been performed using a mild oxidizing agent such as CAT, which decomposes to hypochlorite anion that acts as an oxidizing agent, transforming iodine from  $\text{I}^-$  to the oxidative state  $\text{I}^+$ . The radioiodination of TZN is highly dependent on the concentration of CAT. Fig. (3) shows that the radiochemical yield of  $^{125}\text{I}$ -TZN increased to  $92.8 \% \pm 0.1$  at 50  $\mu\text{g}$  CAT. Increasing the CAT amount above 50  $\mu\text{g}$  led to a decrease in the radioiodination yield due to the formation of undesirable oxidative by-products like chlorination, polymerization and denaturation of TZN [19].

#### *Effect of reaction temperature*

The radioiodination of TZN was carried out by studying the effect of the reaction temperature (25-100 °C) using 100  $\mu\text{g}$  TZN and 50  $\mu\text{g}$  CAT at pH 7

for 15 min. The data indicated that the reaction temperature is a significant factor that affects the labeling yield. Fig. (4) shows that the maximum radiochemical yield was 94.4 % at 80 °C. Nevertheless, there was no need to raise the reaction temperature to such a high temperature while the radiochemical yield was good enough at room temperature (92.8 %  $\pm$  0.1) and too close to the maximum yield. Hence, room temperature was considered the optimum temperature.

#### Effect of pH of reaction medium

The variation of the radiochemical yield of  $^{125}\text{I}$ -TZN with CAT as a function of pH was investigated in the pH range from 2 to 11. Fig. (5) shows that the maximum radiochemical yield of

$^{125}\text{I}$ -TZN (92.8 %  $\pm$  0.1) was obtained at pH 7. At acidic pH, the radiochemical yield of  $^{125}\text{I}$ -TZN decreased and this may be attributed to the predominance of  $\text{ICl}$  species which have low oxidation potential less than  $\text{HOCl}$  [20]. At alkaline pH, the yield also decreased markedly reaching 36.2 %, as a result of decreasing  $\text{HOI}$  which was responsible for the electrophilic substitution reaction.

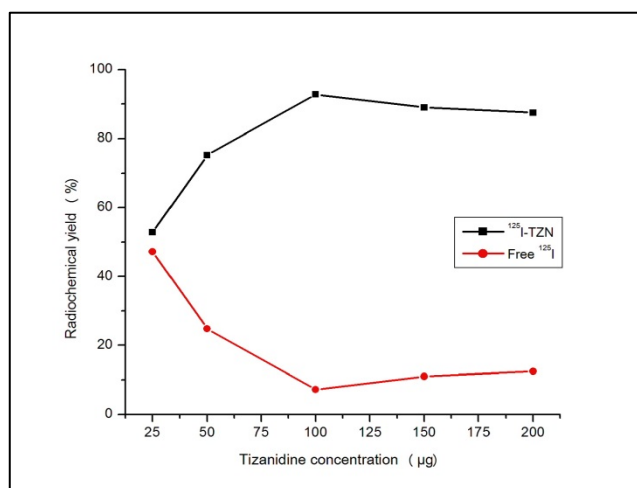


Fig. (2): The radiochemical yield of  $^{125}\text{I}$ -TZN as a function of substrate amount (x µg TZN, 50 µg CAT, about 3.7 MBq  $\text{Na}^{125}\text{I}$ , pH 7, at room temperature for 15 min)

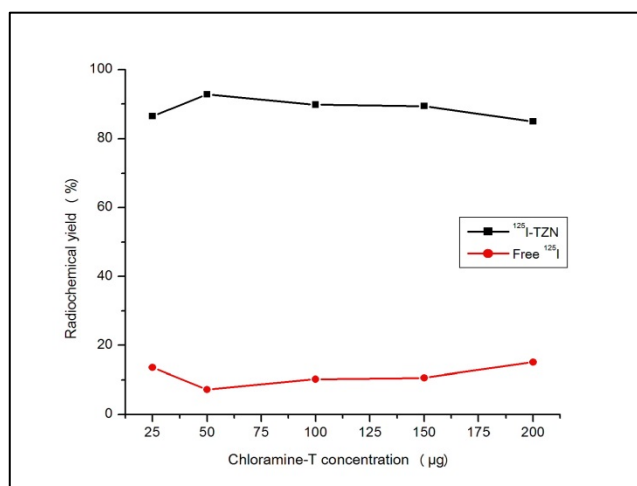


Fig. (3): The radiochemical yield of  $^{125}\text{I}$ -TZN as a function of CAT amount (100 µg TZN, x µg CAT, about 3.7 MBq  $\text{Na}^{125}\text{I}$ , pH 7, at room temperature for 15 min)

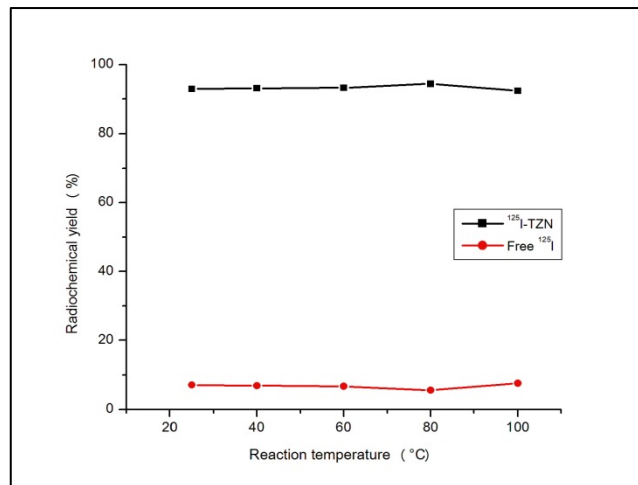


Fig. (4): Effect of temperature on the radiochemical yield of  $^{125}\text{I}$ -TZN (100  $\mu\text{g}$  TZN, 50  $\mu\text{g}$  CAT, about 3.7 MBq  $\text{Na}^{125}\text{I}$ , pH 7, at x  $^{\circ}\text{C}$  for 15 min)

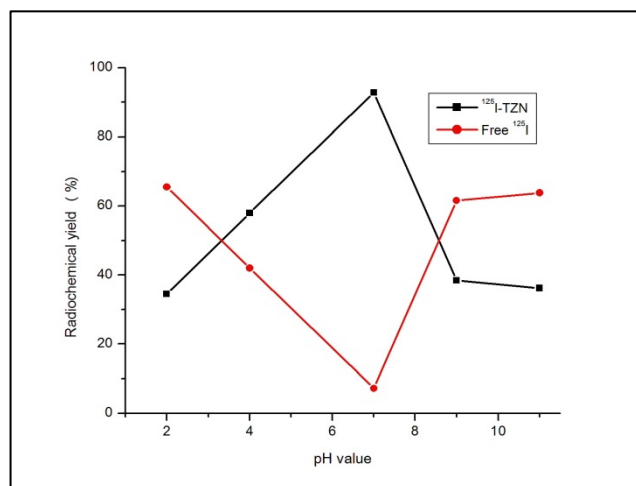


Fig. (5): Effect of pH on the radiochemical yield of  $^{125}\text{I}$ -TZN (100  $\mu\text{g}$  TZN, 50  $\mu\text{g}$  CAT, about 3.7 MBq  $\text{Na}^{125}\text{I}$ , pH x, at room temperature for 15 min)

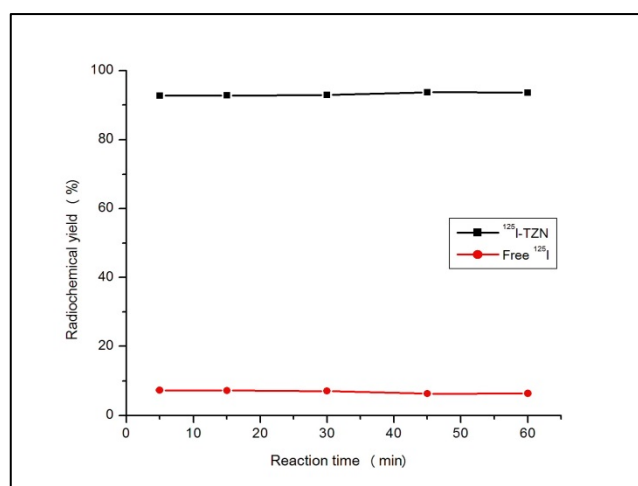


Fig. (6): The radiochemical yields of  $^{125}\text{I}$ -TZN as a function of reaction time (100  $\mu\text{g}$  TZN, 50  $\mu\text{g}$  CAT, about 3.7 MBq  $\text{Na}^{125}\text{I}$ , pH 7, at room temperature for x min)

#### Effect of reaction time

It is clear from Fig. (6) that the radiochemical yield increased with time till reaching 93.7 % after 45 min, but this was considered a time consuming. Thus, only 15 min with 92.8 %  $\pm$  0.1 radiochemical yield would be sufficient for radiolabeling procedure and considered the optimum reaction time.

#### In vitro stability

The stability of  $^{125}\text{I}$ -TZN was studied in order to determine the suitable period of injection to avoid the formation of undesired products which would result from the radiolysis of the labeled compound. Table (1) shows that  $^{125}\text{I}$ -TZN is stable for 2 h and its storage for a long time (24 h) causes its decomposition and a decrease of its yield to 75.9 %.

#### Lipophilicity

The partition coefficient value of  $^{125}\text{I}$ -TZN was  $2.21 \pm 0.02$ , showing that  $^{125}\text{I}$ -TZN is very lipophilic and can easily cross the blood-brain barrier to the target receptors.

#### HPLC analysis

A radiochromatogram for  $^{125}\text{I}$ -TZN obtained after HPLC separation on RP-C18 column at optimum conditions is shown in Fig. (7). Three peaks were obtained; the first peak at 2 min corresponds to TZN while the second peak at 5 min corresponds to the free iodide and the third peak at 12 min corresponds to  $^{125}\text{I}$ -TZN. The eluted fractions containing the labeled compound were pooled together and evaporated to dryness. The residue

was dissolved in physiological saline and sterilized by filtration through 0.22  $\mu\text{m}$  Millipore filter, and the  $^{125}\text{I}$ -TZN is then suitable for use in biodistribution studies and SPECT imaging.

Table (1): In vitro stability of  $^{125}\text{I}$ -TZN at optimum labeling conditions (100  $\mu\text{g}$  TZN, 50  $\mu\text{g}$  CAT, about 3.7 MBq  $\text{Na}^{125}\text{I}$ , pH 7, at room temperature for 15 min)

Time post labeling (h)	$^{125}\text{I}$ -TZN labeling yield (%)
1	$90.2 \pm 0.3$
2	$89.9 \pm 1.0$
4	$76.5 \pm 0.2$
8	$76.1 \pm 0.2$
24	$75.9 \pm 0.9$

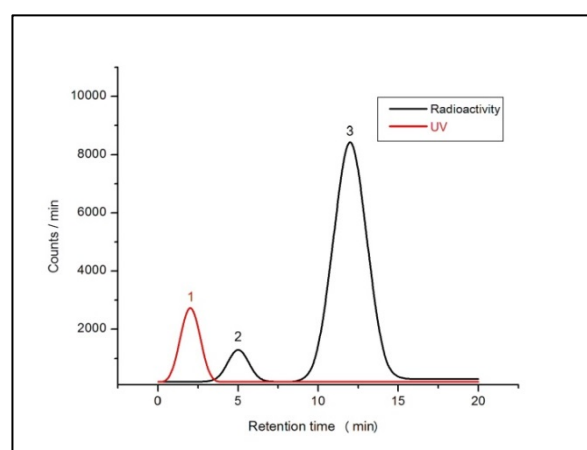


Fig. (7): HPLC elution profile of  $^{125}\text{I}$ -TZN mixture at optimum labeling conditions (peak (1) for TZN, peak (2) for  $\text{Na}^{125}\text{I}$ , peak (3) for  $^{125}\text{I}$ -TZN)

#### Biodistribution studies

Biodistribution study of  $^{125}\text{I}$ -TZN in normal mice showed high brain uptake (1.7 %) at 10 min post injection, indicating the ability of the tracer to penetrate the blood-brain barrier as fast as the tracer injected. The clearance rate from the brain tissues was slow, as shown in Table (2), indicating that the tracer was bound to  $\alpha_2$ -adrenergic receptors in the brain. The renal uptake is higher than the hepatic uptake indicating that the labeled compound excreted mainly through the urinary system. The low activity located in the thyroid gland indicates that  $^{125}\text{I}$ -TZN is stable *in vivo* against biological decomposition. The ability and the efficiency of the labeled compound to be used as a brain imaging agent depends greatly on the ratio of the activity hold by the brain to the background activity (blood activity). The high brain-to-blood ratio, which is due to the high blood clearance, makes the radiolabeled TZN suitable for use as a brain-imaging agent.

#### *In vivo SPECT imaging*

*In vivo* SPECT brain scans of Albino mouse injected with  $^{131}\text{I}$ -TZN were shown in Fig. (8) in order to visualize the drug localization in the brain. These images were taken at four different time intervals (10, 60, 120 and 240 min post intravenous injection), but it was not highly clear due to the small size of the mouse (a mouse is ~ 3000 times smaller in weight than a human). After

10 min of injection, there was a significant  $^{131}\text{I}$ -TZN percentage reached to the brain (1.8 %), and it increased to the maximum (8.0 %) after 120 min post injection, then decreased again to 5.1 % after 240 min of injection as shown in Table (3).

#### **Conclusion**

TZN was labeled with radioactive iodine by direct electrophilic substitution reaction and the produced tracer was evaluated radiochemically to select the optimum conditions required to produce a high radiolabeling yield. TZN was efficiently labeled with a radiochemical yield of  $92.8\% \pm 0.1$  when its amount was 100  $\mu\text{g}$  in the presence of 50  $\mu\text{g}$  CAT as oxidizing agent at pH 7 and the reaction mixture was incubated for 15 min at room temperature. The radiolabeled TZN was intravenously injected in mice and the brain uptake was 5.2 % and 8.0 % at 120 min post injection in biodistribution studies and SPECT imaging, respectively, which indicates that this labeled compound can be used as a radiopharmaceutical imaging agent.

**Table (2): Biodistribution of  $^{125}\text{I}$ -TZN (in %) in normal mice at different time intervals**

Organs and body fluids	Time post injection(min)			
	10	60	120	240
Brain	1.7 $\pm$ 0.5	3.6 $\pm$ 0.3	5.2 $\pm$ 0.2	4.2 $\pm$ 0.1
Blood	17.1 $\pm$ 1.0	9.5 $\pm$ 0.7	9.0 $\pm$ 0.6	7.5 $\pm$ 0.2
Liver	16.1 $\pm$ 0.8	8.8 $\pm$ 0.6	8.3 $\pm$ 0.4	7.6 $\pm$ 0.3
Intestine	12.9 $\pm$ 0.4	18.2 $\pm$ 0.9	11.6 $\pm$ 1.1	9.3 $\pm$ 1.3
Stomach	5.3 $\pm$ 0.4	7.2 $\pm$ 0.7	16.5 $\pm$ 1.0	15.1 $\pm$ 0.5
Lungs	4.4 $\pm$ 0.2	0.4 $\pm$ 0.2	0.5 $\pm$ 0.1	0.7 $\pm$ 0.1
Heart	1.3 $\pm$ 0.1	0.4 $\pm$ 0.1	0.4 $\pm$ 0.1	0.4 $\pm$ 0.1
Kidneys	13.5 $\pm$ 0.3	10.4 $\pm$ 0.4	9.2 $\pm$ 0.4	9.6 $\pm$ 0.2
Spleen	2.9 $\pm$ 0.1	0.2 $\pm$ 0.1	0.2 $\pm$ 0.1	0.3 $\pm$ 0.1
Muscles	7.5 $\pm$ 0.3	6.9 $\pm$ 0.4	4.0 $\pm$ 0.2	4.4 $\pm$ 0.2
Bones	1.3 $\pm$ 0.3	6.9 $\pm$ 0.2	5.8 $\pm$ 0.1	8.7 $\pm$ 0.1
Thyroid	0.1 $\pm$ 0.05	0.1 $\pm$ 0.05	0.1 $\pm$ 0.05	0.1 $\pm$ 0.05
Urine	16.0 $\pm$ 0.8	27.3 $\pm$ 0.6	29.2 $\pm$ 1.2	32.1 $\pm$ 2.4
Brain*	4.3 $\pm$ 0.5	9.6 $\pm$ 0.3	13.2 $\pm$ 0.2	9.7 $\pm$ 0.1
Blood*	10.7 $\pm$ 1.0	6.4 $\pm$ 0.7	5.5 $\pm$ 0.6	5.0 $\pm$ 0.2
(Br/Bl)*	0.4	1.5	2.4	1.9

\* % Injected dose / g tissue; Br: Brain; Bl: Blood

**Table (3): The injected dose percentage of  $^{131}\text{I}$ -TZN in some organs according to SPECT imaging**

Organs	Time post injection (min)			
	10	60	120	240
Brain	1.8	5.5	8.0	5.1
Liver	5.1	19.9	39.4	25.3
Bladder	2.1	10.4	14.3	7.4

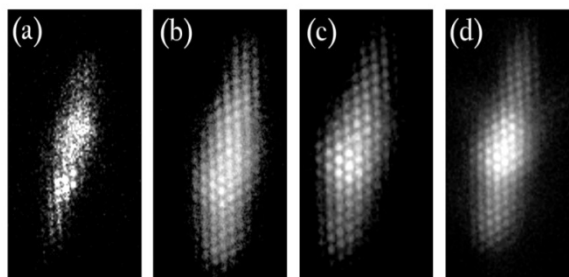


Fig. (8): SPECT brain scan of a mouse injected with  $^{131}\text{I}$ -TZN at four different time intervals (10, 60, 120 and 240 min from (a) to (d))

### References

- Diksic, M. and Reba, R.C. Radiopharmaceuticals and Brain Pathology Studied with PET and SPECT, *CRC press, Inc., US*(1991).
- Duncan, R. SPECT Imaging of the Brain, *Springer Science & Business Media Dordrecht, UK* (1997).
- Wilbur, D.S. Radiohalogenation of Proteins: An Overview of Radionuclides, Labeling Methods, and Reagents for Conjugate Labeling, *Bioconjug. Chem.*, 3, 433-470(1992).
- Stocklin, G. Bromine-77 and Iodine-123 Radiopharmaceuticals, *Appl. Radiat. Isot.*, 28, 131-148(1977).
- Coenen, H.H., Mertens, J. and Maziere, B. Radioiodination Reactions for Pharmaceuticals, *Springer Netherlands*(2006).
- Sanad, M.H. and Challan, S.B. Radioiodination and Biological Evaluation of Rabeprazole as a Peptic Ulcer Localization Radiotracer, *Radiochemistry*, 59 (3), 307-312(2017).
- Kumar, C., Subramaniam, S. and Samuel, G. Evaluation of Radioiodinated Curcumin for its Potential as a Tumor-Targeting Radiopharmaceutical, *J. Radiat. Cancer Res.*, 7 (4), 112-116(2016).
- Runnegar, M., Berndt, N., Kong, S.M., Lee, E.Y.C. and Zhang, L.F. *In Vivo* and *In Vitro* Binding of Microcystin to Protein Phosphatase 1 and 2A, *Biochem. Biophys. Res. Commun.*, 216 (1), 162-169(1995).
- Park, J.J., Lee, T.S., Kang, J.H., Song, R. and Cheon, G.J. Radioiodination and Biodistribution of Quantum Dots using Bolton–Hunter Reagent, *Appl. Radiat. Isot.*, 69 (1), 56-62(2011).
- Malmberg, J., Strandgard, J., Tolmachev, V., Orlova, A. and Andersson, K. Protein Interactions with the HER2 Receptor can have Different Characteristics Depending on the Hosting Cell-Line, *J. Nucl. Med.*, 53 (1), 1713(2012).
- Reist, C.J., Archer, G.E., Kurpad, S.N., et al, Tumor-Specific Anti-Epidermal Growth Factor Receptor Variant III Monoclonal Antibodies: Use of the Tyramine-Cellobiose Radioiodination Method Enhances Cellular Retention and Uptake in Tumor Xenografts, *Cancer Res.*, 55 (19), 4375-4382(1995).
- Cheng, F., Li, W., Zhou, Y., Shen, J., Wu, Z., Liu, G., Lee, P.W. and Tang, Y. admetSAR: A Comprehensive Source and Free Tool for Assessment of Chemical ADMET Properties, *J. Chem. Inf. Model.*, 52 (11), 3099-3105(2012).
- Coenen, H.H., Moerlein, S.M. and Stocklin, G. No-Carrier-Added Radiohalogenation Methods with Heavy Halogens, *Radiochim. Acta*, 34, 47-68(1983).
- Greenwood, N. and Earnshaw, A. Chemistry of the Elements, 2<sup>nd</sup> Ed., *Butterworth-Heinemann, Oxford*(1997).
- Nimje, H., Wate, S.P., Dharkar, D.P. and Razdan, R. Simultaneous RPHPLC Determination of Nimesulide and Tizanidine in Tablets, *Indian J. Pharm. Sci.*, 69 (2), 281-283(2007).
- Liu, F.E.I., Youfeng, H.E. and Luo, Z. Study of  $^{99\text{m}}\text{Tc}$  Labelled Way Analogues for 5-HT<sub>1A</sub> Receptor Imaging, *IAEA, Technical Reports Series No. 426*, 37(2004).
- Amin, A.M., Sanad, M.H. and Abd-Elhaliem, S.M. Radiochemical and Biological Characterization of  $^{99\text{m}}\text{Tc}$ -Piracetam for Brain Imaging, *Radiochemistry*, 55 (6), 624-628(2013).
- El-Azony, K.M., El-Mohty, A.A., Killa, H.M., Seddik, U. and Khater, S.I. (2009) An Investigation of the  $^{125}\text{I}$ -radioiodination of Colchicine for Medical Purposes, *J. Labelled Compd. Rad.*, 52 (1), 1-5.
- El-Azony, K.M. Preparation of  $^{125}\text{I}$ -celecoxib with High Purity as a Possible Tumor Agent, *J. Radioanal. Nucl. Ch.*, 285 (2), 315-320(2010).



- 
- 20- Bearer, C.F., Knapp, R.D., Kaumann, A.J., Swartz, T.L. and Birnbaumer, L. Iodoxybenzylpindolol: Preparation, Purification, Localization of its Iodine to the Indole Ring, and Characterization as a Partial Agonist, *Mol. Pharmacol.*, 17 (3), 328-338(1980).